Unusual Square Pyramidal Chalcogenide Mo₅ Cluster with Bridging Pyrazolate-Ligands

Iulia V. Savina [1], Anton A. Ivanov [1,*], Darya V. Evtushok [1], Yakov M. Gayfulin [1], Andrey Y. Komarovskikh [1], Mikhail M. Syrokvashin [1], Mariia N. Ivanova [1], Igor P. Asanov [1], Ilia V. Eltsov [2], Natalia V. Kuratieva [1], Yuri V. Mironov [1,*] and Michael A. Shestopalov [1]

[1] Nikolaev Institute of Inorganic Chemistry of Siberian Branch of Russian Academy of Sciences, 3 Acad. Lavrentiev ave., 630090, Novosibirsk, Russia

[2] Department of Natural Sciences, Novosibirsk State University, 1 Pirogova st., 630090, Novosibirsk, Russia

*Correspondence: ivanov338@niic.nsc.ru (A.A.I.), yuri@niic.nsc.ru (Y.V.M.)

# TABLE OF CONTENT

Powder X-ray diffraction analysis

Figure S1. XRPD pattern of **Mo₅red** in comparison with calculated one from the SCXRD data.

UV-vis spectroscopy

Figure S2. UV-vis spectra of **Mo₅red** acetonitrile (a) or DCM (b) solutions in time in comparison with **Mo₅ox**.

Mo₅red: packing in crystal structure
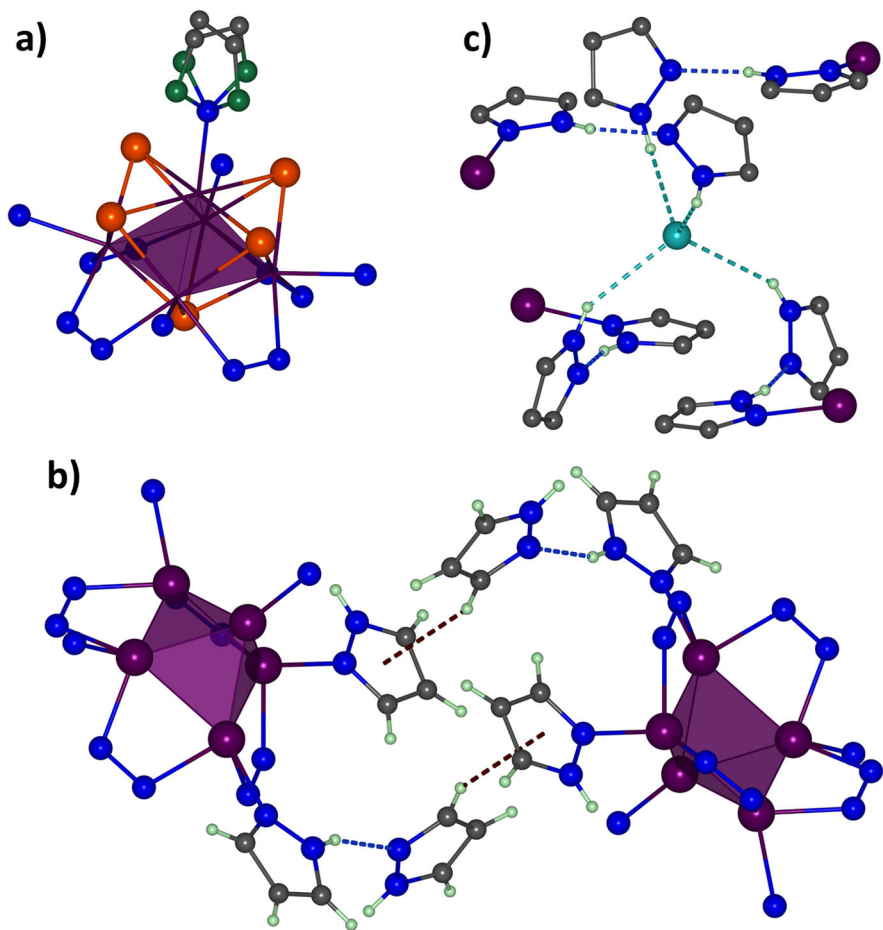
Figure S3. Packing in the crystal structure of **Mo₅red**. a) Disorder of axial pyrazole ligand over four positions. b) Hydrogen bonds and C-H···π stacking interactions between solvated pyrazole molecules and pzH-ligands. c) Hydrogen bonds between bromine-ion and solvated pyrazole molecules. Color code: Mo – violet, Mo₅ – violet square pyramid, C – gray, N – blue, Br – cyan, H – light green, disordered C/N – green, C-H···π – red, N-H···N – blue, N-H···Br – cyan.
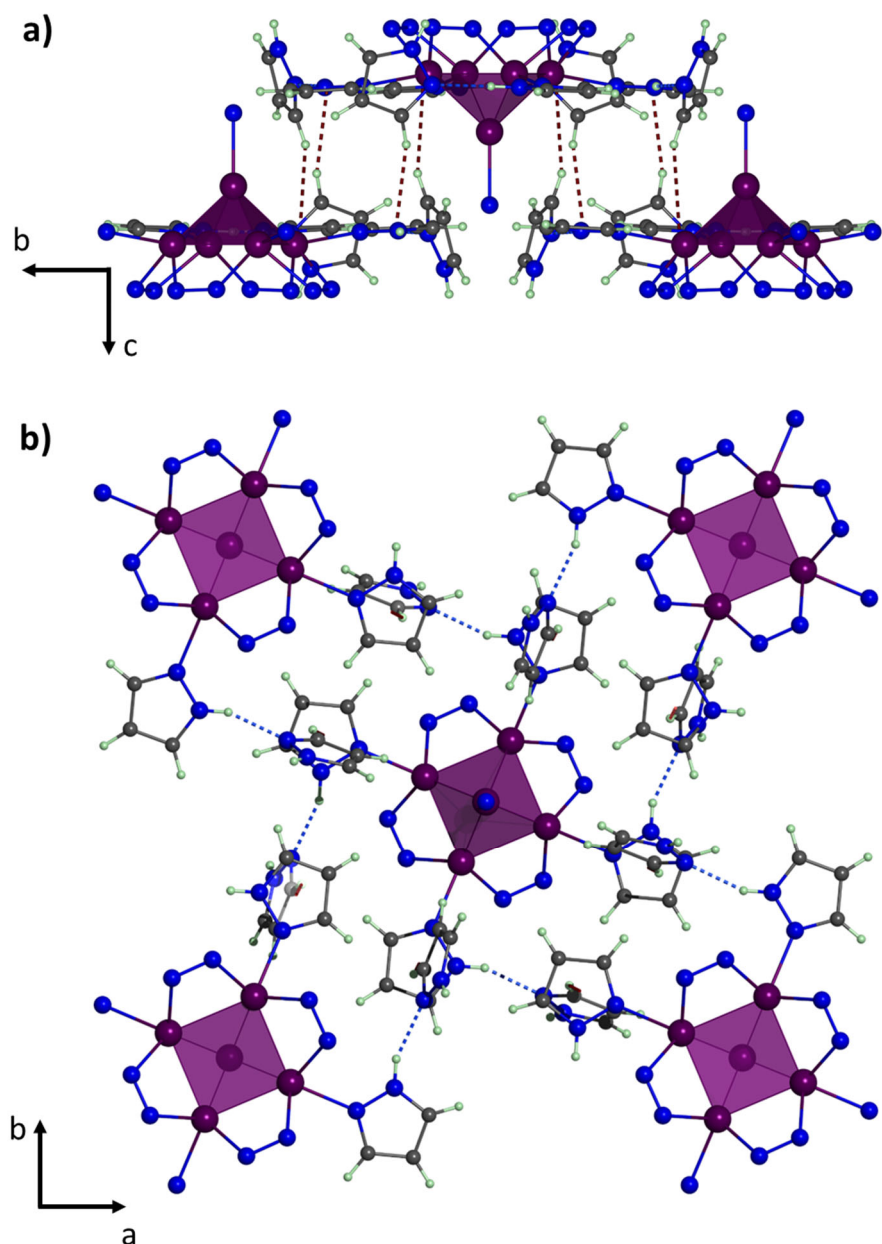
Figure S4. Packing in the crystal structure of **Mo₅red**. Hydrogen bonds and C-H···π stacking interactions between solvated pyrazole molecules and pzH-ligands along *a* (a) and *c* (b) axis. Color code: Mo – violet, Mo₅ – violet square pyramid, C – gray, N – blue, Br – cyan, H – light green, disordered C/N – green, C-H···π – red, N-H···N – blue, N-H···Br – cyan.
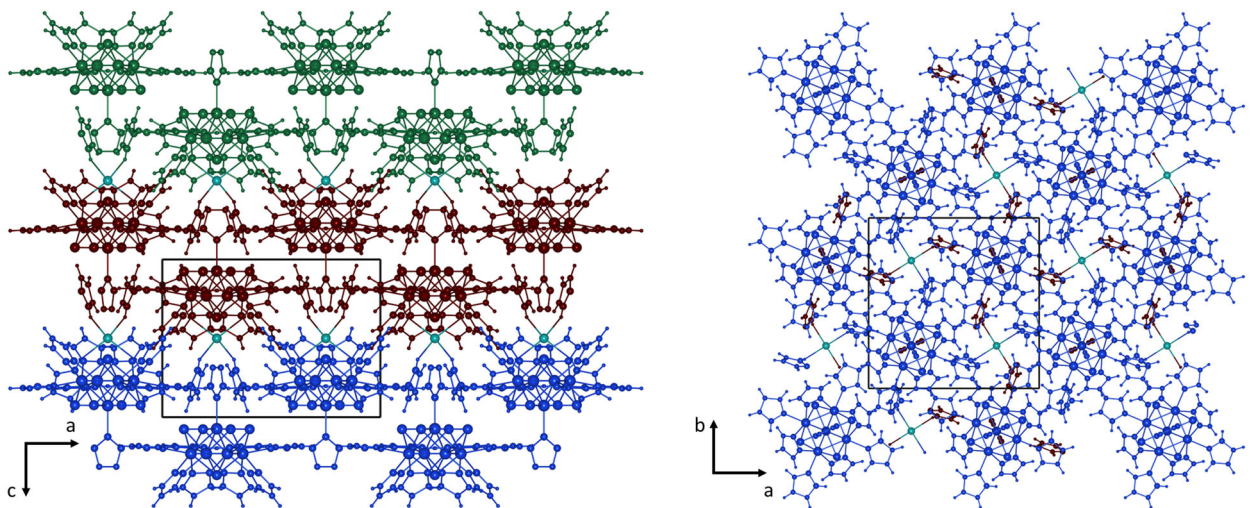
Figure S5. Packing of layers in the crystal structure of **Mo₅red**: side (left) and top (right) view.

Mo₅ox: packing in crystal structure and powder X-ray diffraction analysis
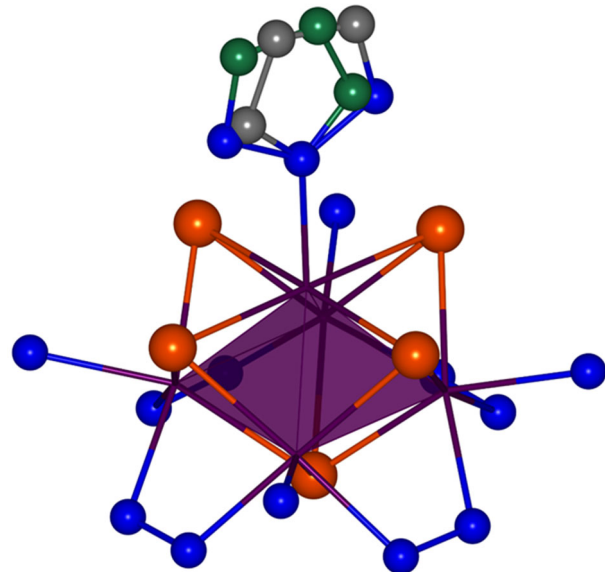

Figure S6. Disorder of axial pyrazole ligand over two positions in the crystal structure of **Mo₅ox**. Color code: Mo – violet, Mo₅ – violet square pyramid, C – gray/green, N – blue.

a)

b)
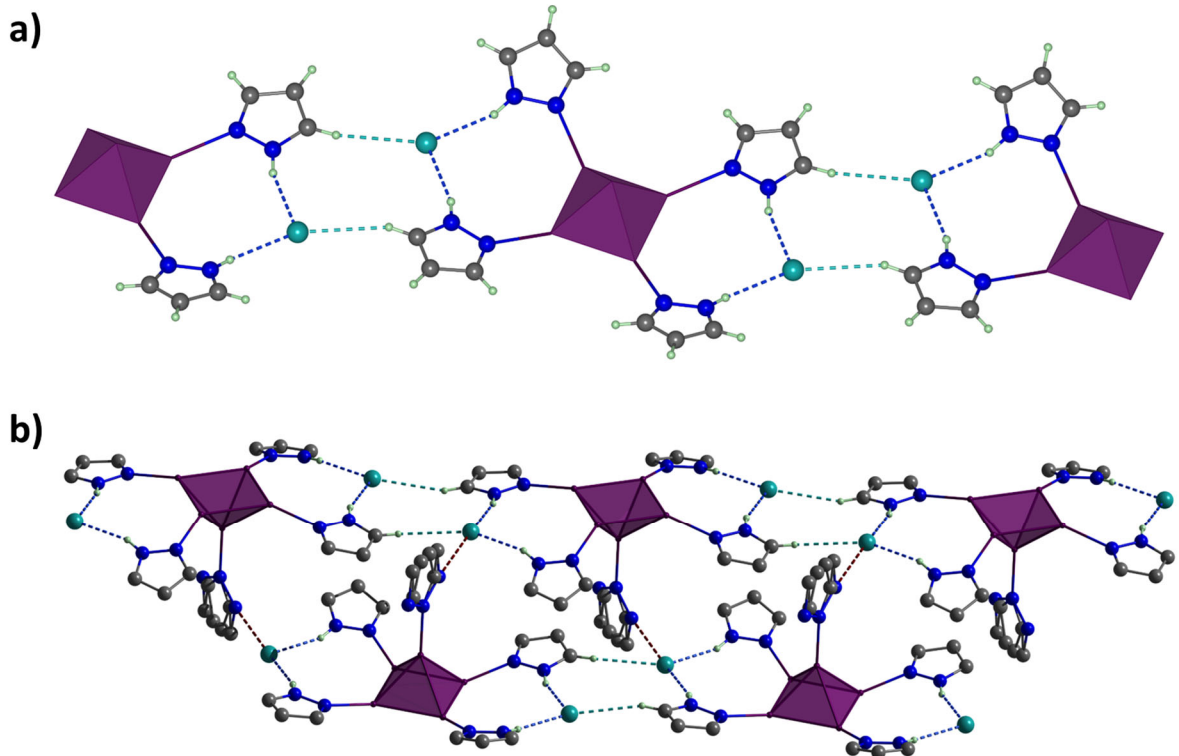
Figure S7. Packing in the crystal structure of **Mo₅ox**. a) Hydrogen bonds between terminal pyrazole ligands and Br forming infinite chains. b) Hydrogen bonds between bromine-ion and axial pyrazoles connecting chains. Color code: Mo – violet, Mo₅ – violet square pyramid, C – gray, N – blue, Br – cyan, H – light green, C-H···Br – cyan, N^{eq}-H···Br – blue, N^{ax}-H···Br – red.
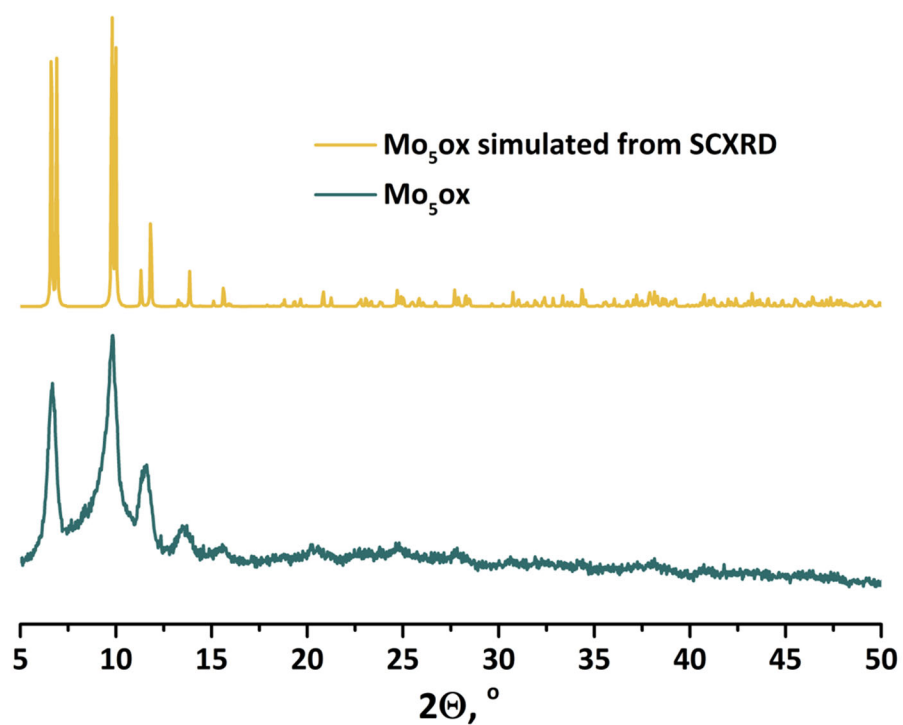
**Figure S8**. XRPD pattern of **Mo₅ox** in comparison with calculated one from the SCXRD data.

DFT calculations

Table S1. Optimized bond lengths (range | average) within the $[Mo_5(\mu_4\text{-Se})(\mu_3\text{-Se})_4(\mu\text{-pz})_4pz_5]^{2+/1+}$ clusters at VWN/S12g/TZP level of theory and C_1 point symmetry.

Cluster / Bond	Mo_{eq}–Mo_{eq}	Mo_{eq}–Mo_{ap}	Mo_{eq}–(μ_3-Se)	Mo_{ap}–(μ_3-Se)	Mo_{eq}–(μ_4-Se)	Mo–N (apical pz)	Mo–N (μ-pz)
$[Mo_5(\mu_4\text{-Se})(\mu_3\text{-Se})_4(\mu\text{-pz})_4pz_5]^+$	2.8430–2.8440 2.8435(6)	2.681–2.686 2.684(2)	2.530–2.550 2.540(8)	2.570–2.585 2.574(8)	2.558–2.561 2.560(1)	2.265–2.273 2.270(3)	2.209–2.215 2.212(2)
$[Mo_5(\mu_4\text{-Se})(\mu_3\text{-Se})_4(\mu\text{-pz})_4pz_5]^{2+}$	2.862–2.872 2.867(5)	2.666–2.669 2.668(1)	2.514–2.531 2.523(7)	2.589–2.594 2.592(2)	2.5600–2.5610 2.5603(5)	2.245–2.262 2.256(7)	2.195–2.204 2.200(4)

Table S2. Orbital energies, symmetry of molecular orbitals and percentage contributions from the metal atoms, selenide ligands and pzH molecules for the $[\{Mo_5(\mu_4\text{-Se})(\mu_3\text{-Se})_4(\mu\text{-pz})_4\}(pzH)_5]^{2+}$ cluster.

MO	Energy (eV)	Mo_5	μ_4-Se	μ_3-Se	μ-pz	Outer pz
352 (LUMO+2)	-2.384	75.43	–	24.57	–	–
351 (LUMO+1)	-3.762	82.12	2.36	8.76	6.76	–
350 (LUMO)	-4.306	67.76	1.29	30.95	–	–
349 (HOMO)	-6.345	79.84	4.98	10.59	3.11	1.48
348 (HOMO-1)	-6.411	87.11	5.64	1.42	5.83	–
347 (HOMO-2)	-6.684	73.71	–	15.65	–	10.64
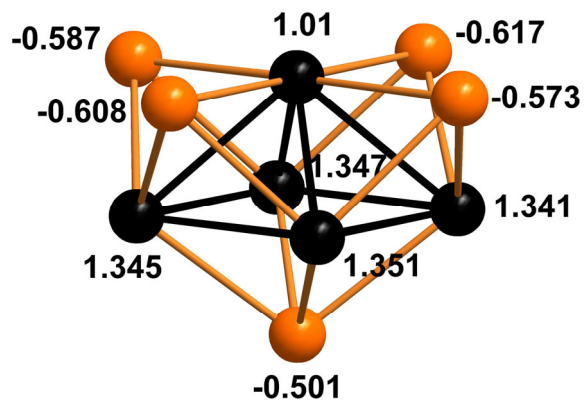
Figure S9. Bader charges on the atoms of the $\{Mo_5Se_5\}$ fragment of the $[\{Mo_5(\mu_4\text{-}Se)(\mu_3\text{-}Se)_4(\mu\text{-}pz)_4\}(pzH)_5]^{2+}$ cluster.
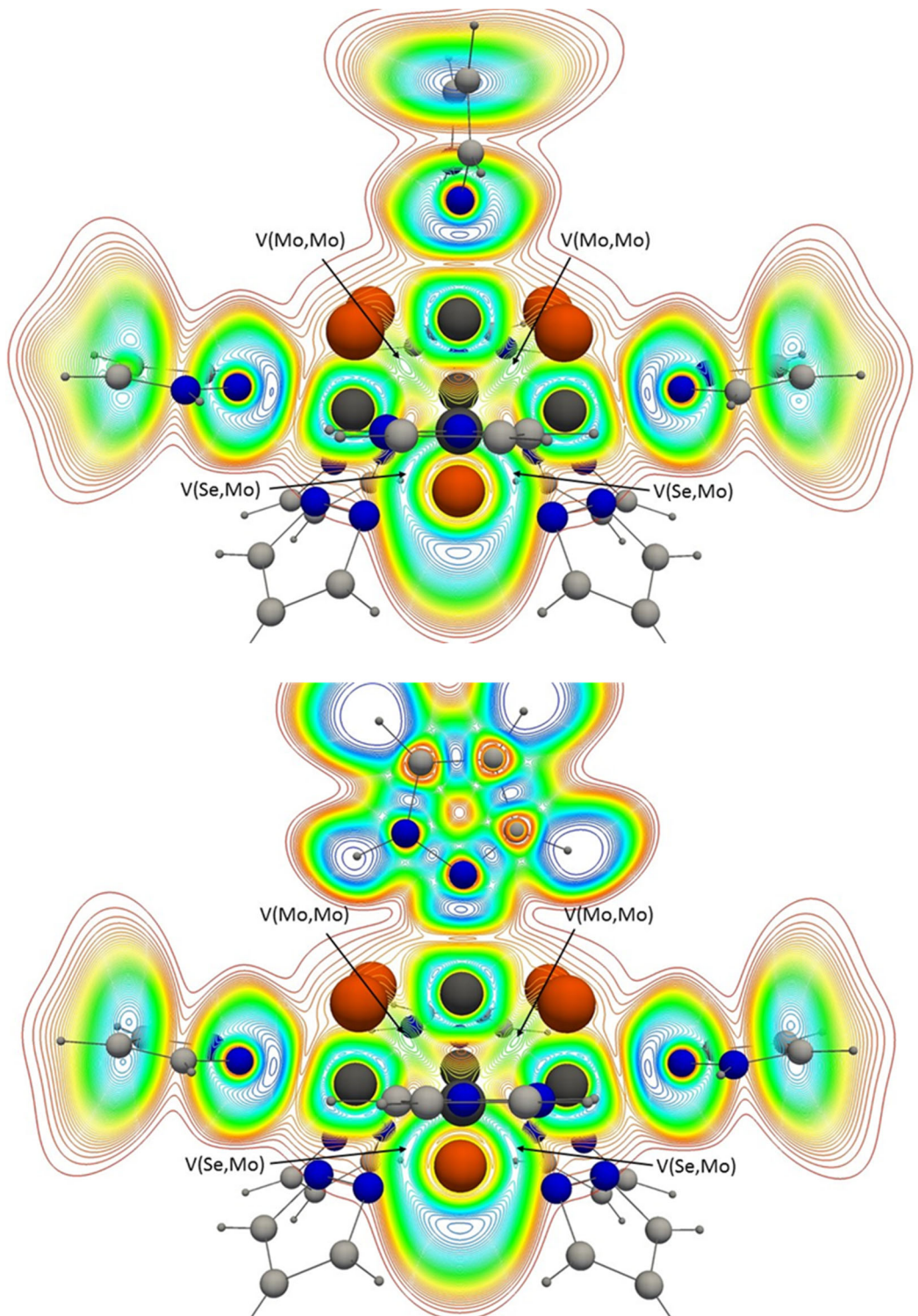
Figure S10. ELF maps for $[\{Mo_5(\mu_4\text{-Se})(\mu_3\text{-Se})_4(\mu\text{-pz})_4\}(pzH)_5]^{2+}$ cluster (cutting planes Mo_{eq}–Mo_{ax}–Mo_{eq}–(μ_4-Se). Color code: Mo, dark gray; Se, orange; N, blue; C, H, light gray. V(Mo,Mo) and V(Se,Mo) are disynaptic basins between corresponding atoms.

XPS data
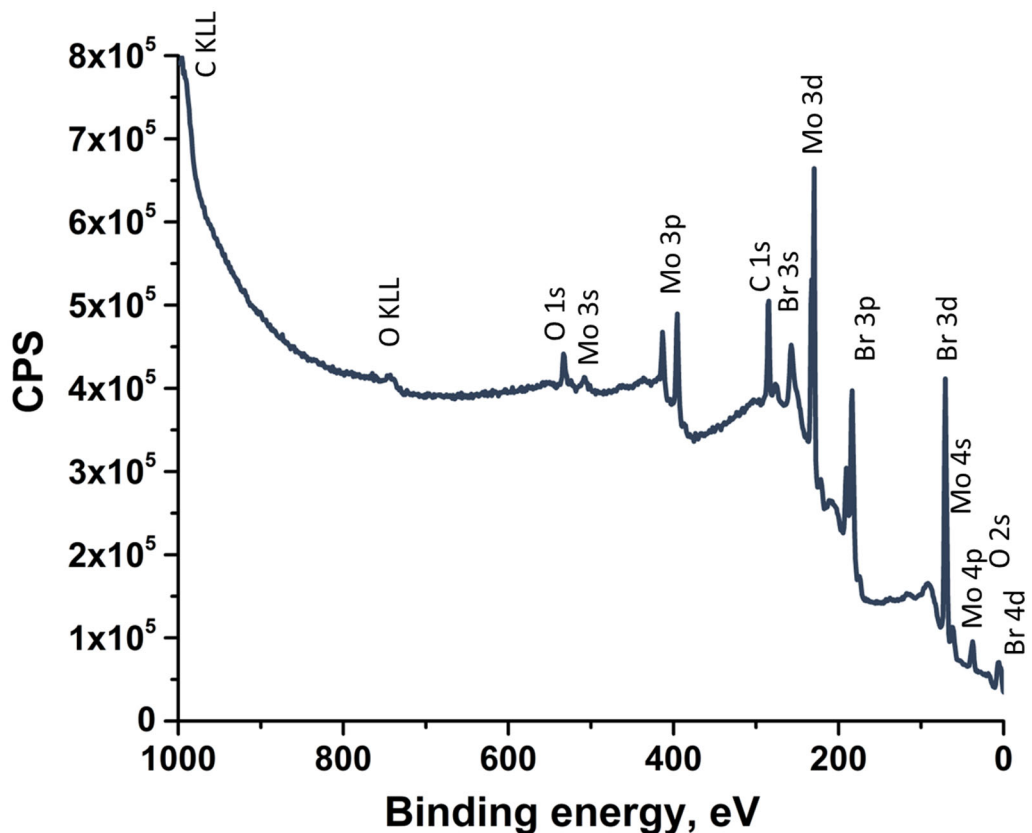
Figure S11. XPS survey spectrum of Mo_6Br_{12}.
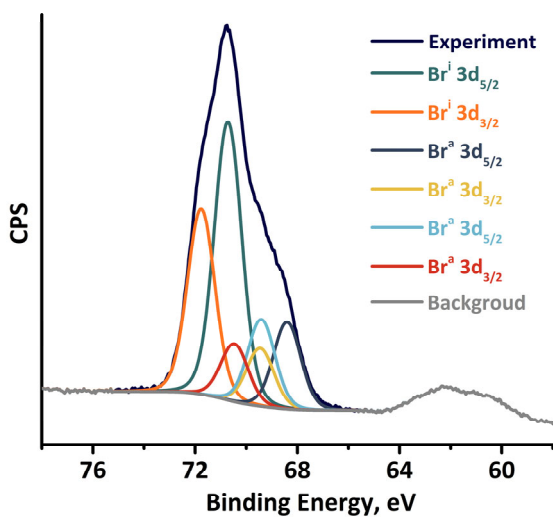
**Figure S12.** XPS spectrum showing Br 3d core level of Mo_6Br_{12}.
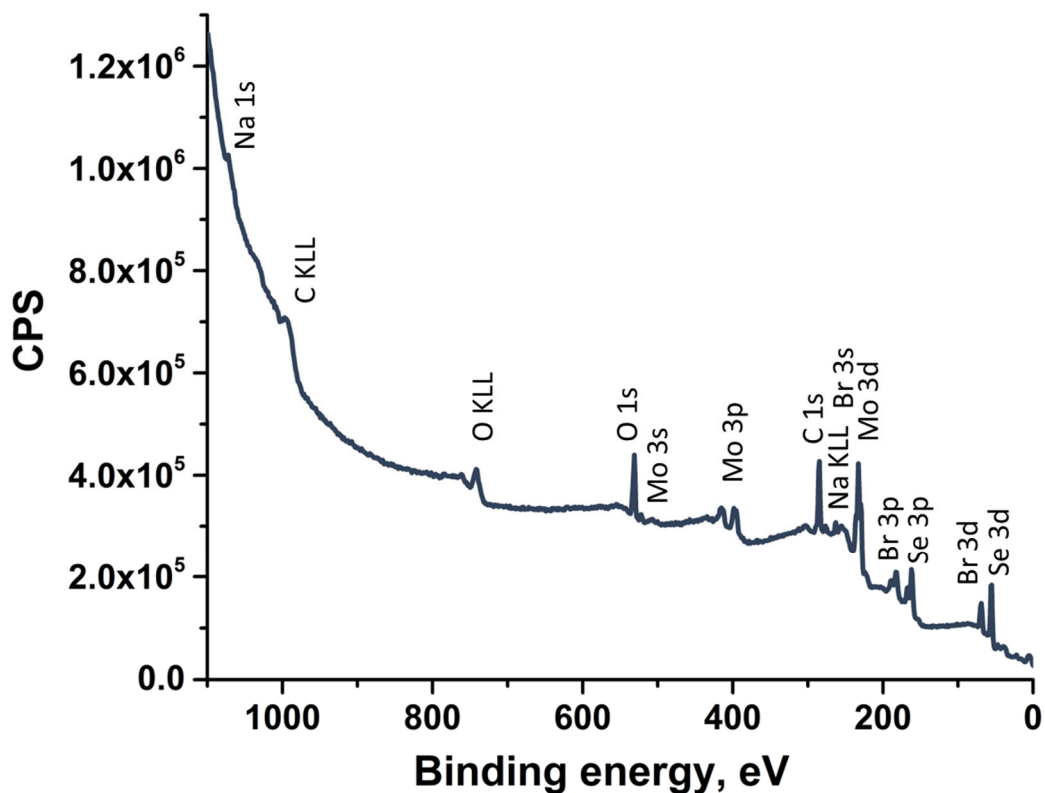
**Figure S13.** XPS survey spectrum of **Mo₆**.
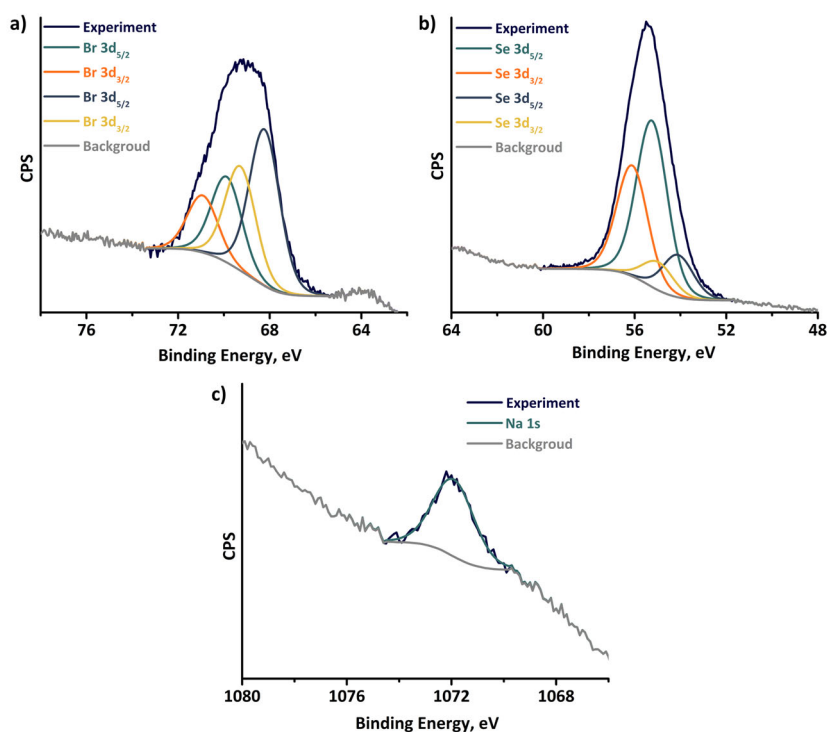
**Figure S14.** XPS spectra showing Br 3d (a), Se 3d (b) and Na 1s (c) core level of **Mo₆**.
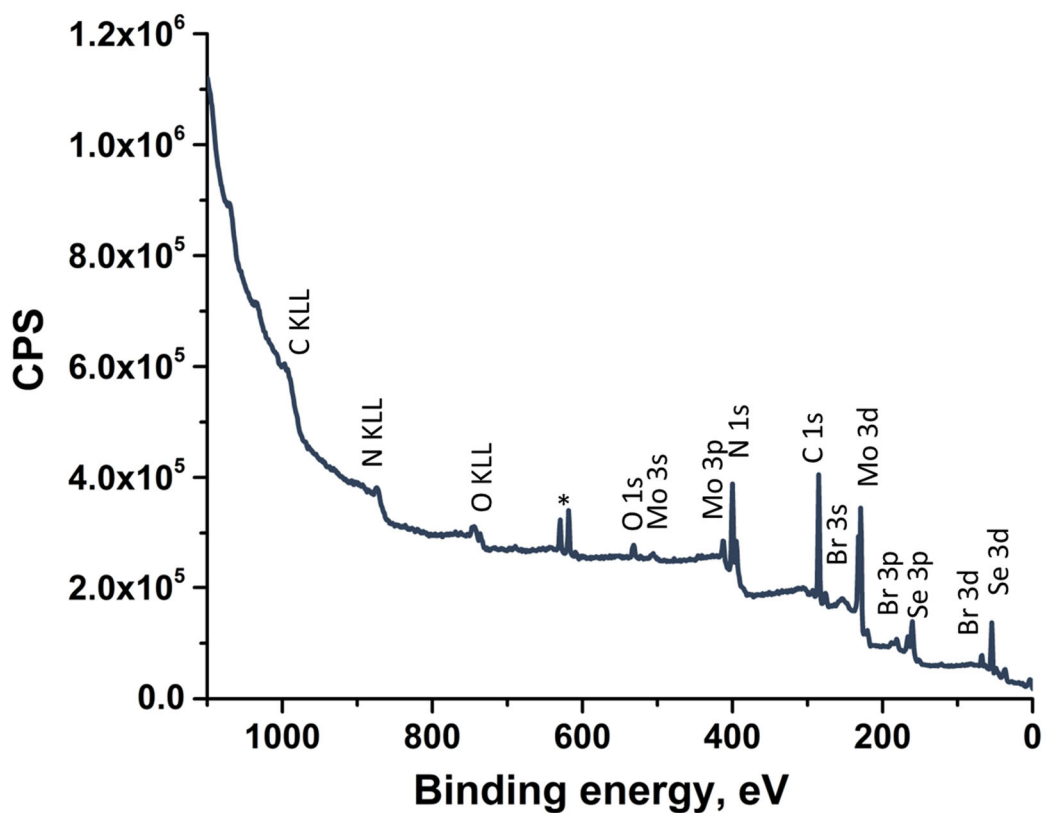
Figure S15. XPS survey spectrum of **Mo$_5$red**.
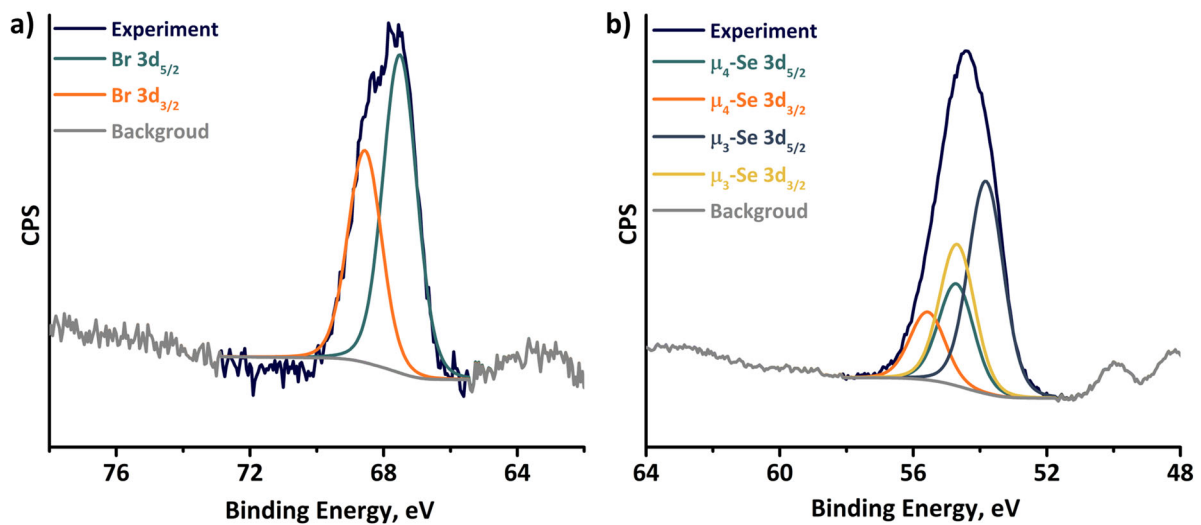
Figure S16. XPS spectra showing Br 3d (a) and Se 3d (b) core level of **Mo$_5$red**.
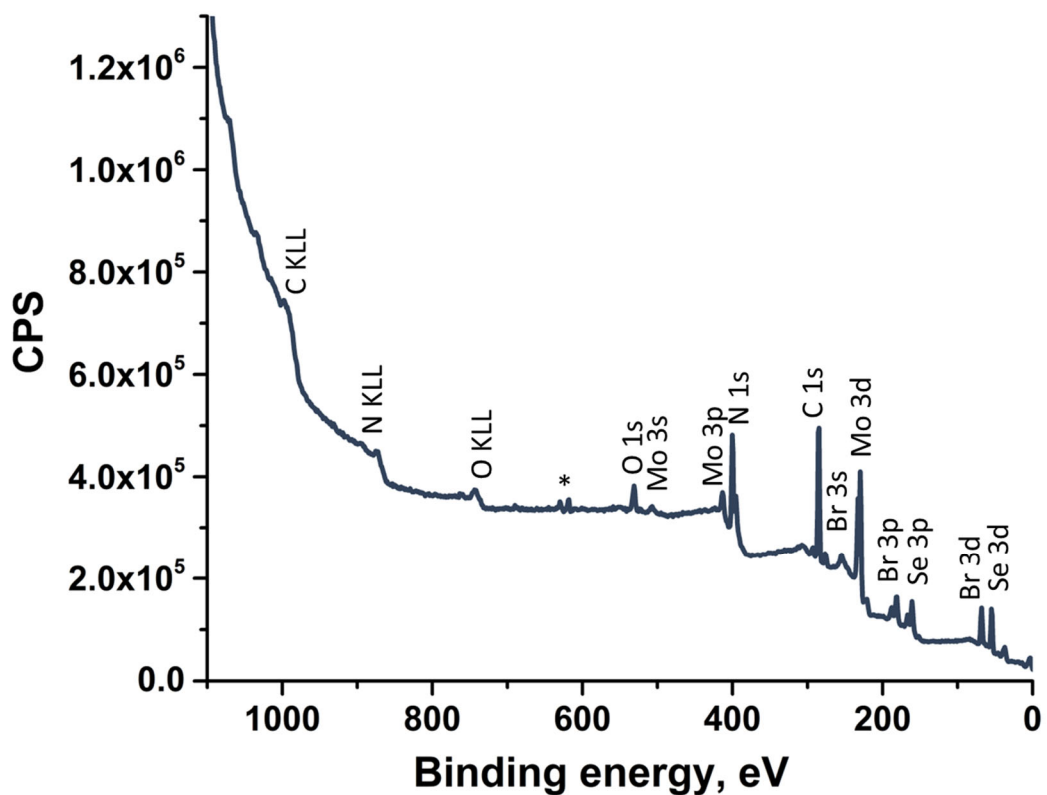
**Figure S17.** XPS survey spectrum of **Mo₅ox**.
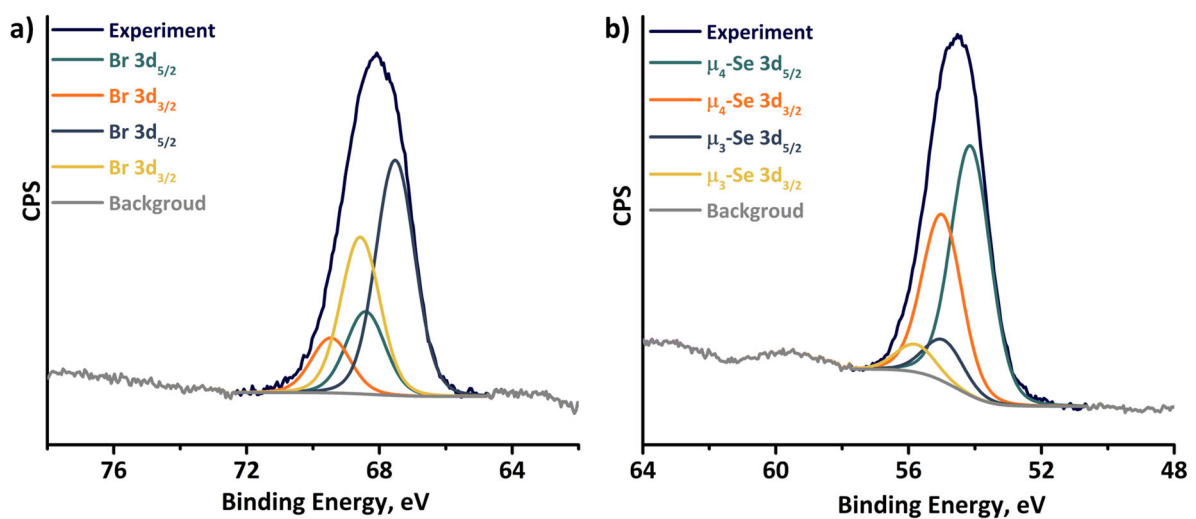
Figure S18. XPS spectra showing Br 3d (a) and Se 3d (b) core level of **Mo₅ox**.

Table S3. XPS binding energies (eV) in clusters obtained.

| Compound	Mo3d$_{5/2,3/2}$ (%)	Br3d$_{5/2,3/2}$ (%)	Se3d$_{5/2,3/2}$ (%)	Na1s
Mo$_6$Br$_{12}$	229.8–232.9 (100%)	68.4-69.5 (19%) 69.4-70.5 (19%) 70.7-71.7 (62%)	–	–
Mo$_6$	229.2–232.4 (54%) 232.8–236.0 (46%)	68.2-69.3 (65%) 69.9-70.9 (35%)	54.1-55.0 (19%) 55.3-56.1 (81%)	1071.9
Mo$_5$red	228.9–232.1 (95%) 231.7–234.8 (4%) 233.3–236.4 (1%)	67.5-68.6	53.8-54.7 (66%) 54.7-55.6 (34%)	–
Mo$_5$ox	229.3–232.4 (78%) 230.7–233.9 (20%) 232.1–235.2 (2%)	67.5-68.6 (74%) 68.4-69.5 (26%)	54.1-55.0 (86%) 54.9-55.8 (14%)	–

NMR spectroscopy data
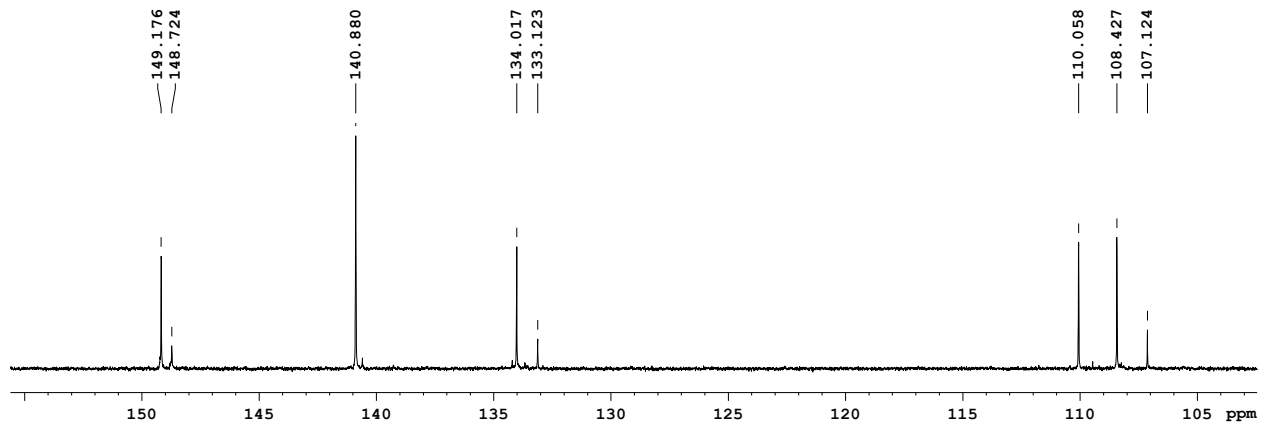
Figure S19. ^{13}C NMR spectrum of **Mo₅ox** in CD₃OD.
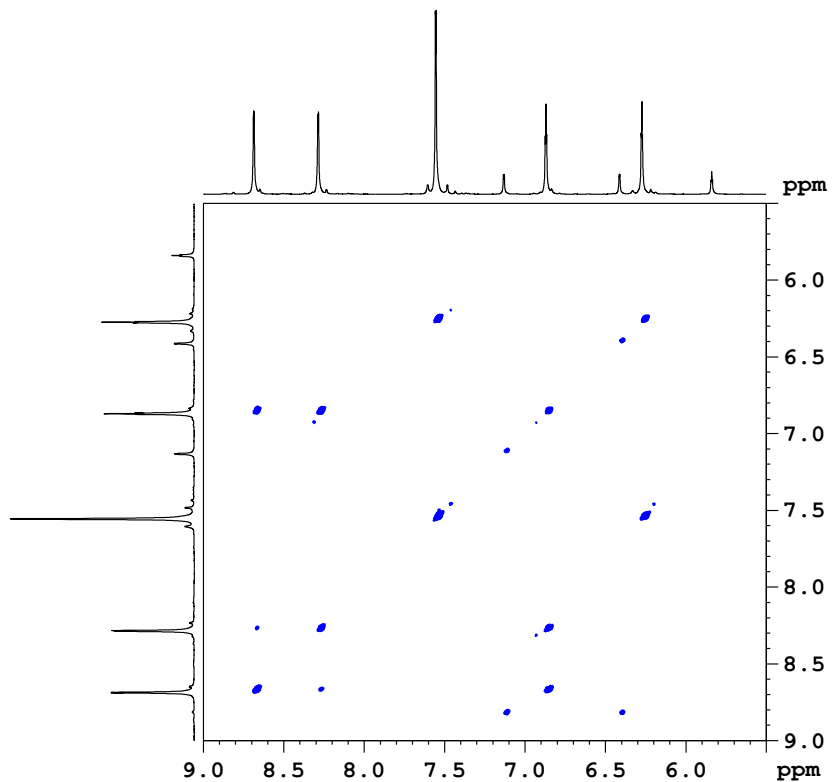
Figure S20. ^{1}H,^{1}H-NMR correlation spectra of **Mo₅ox** in CD₃OD.
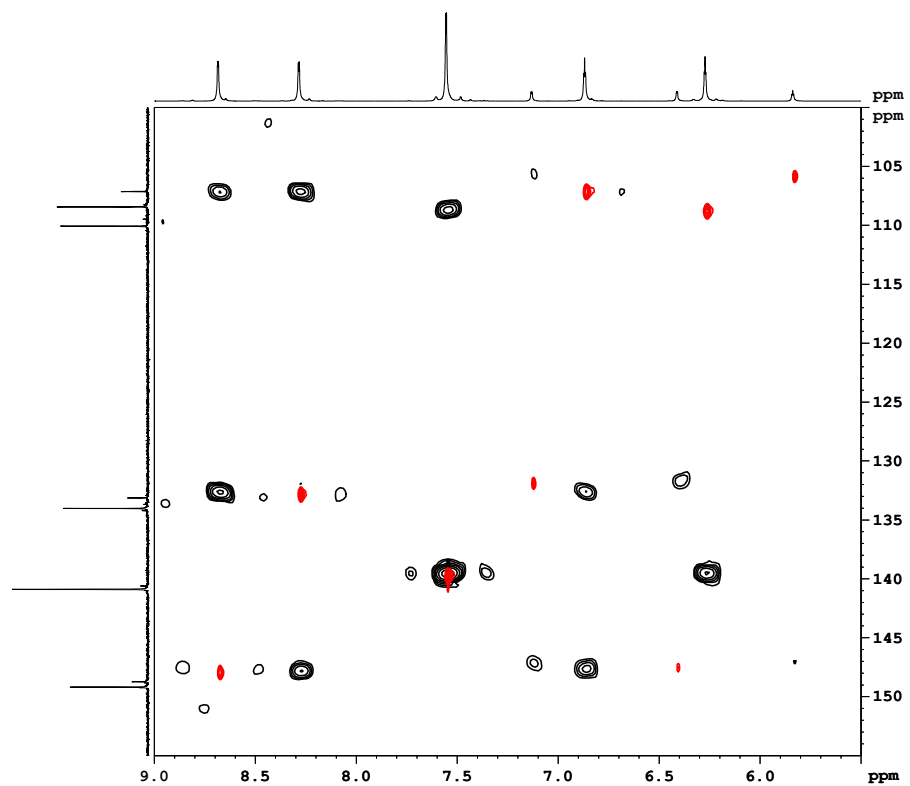
Figure S21. ^{1}H,^{13}C-NMR correlation spectra (HMBC – black, HSQC – red) of **Mo$_5$ox** in CD$_3$OD.
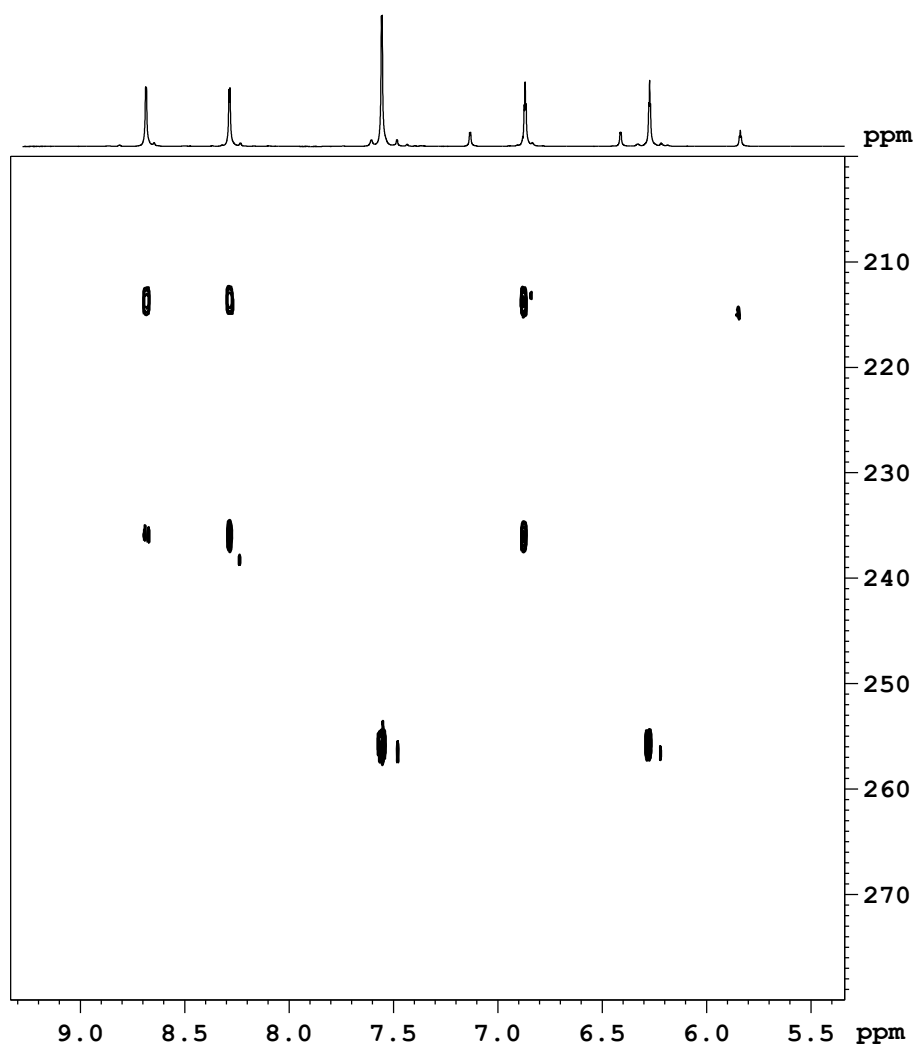
Figure S22. ^{1}H,^{15}N-NMR HMBC spectrum of **Mo₅ox** in CD₃OD.
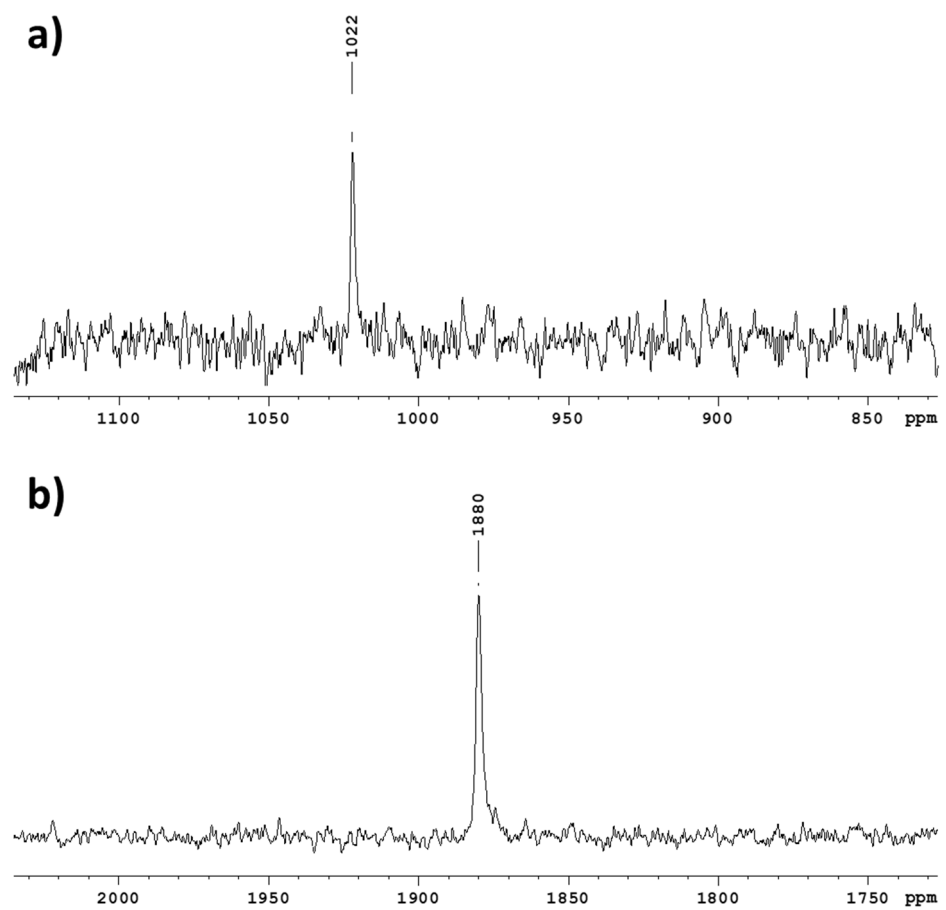
Figure S23. ^{77}Se NMR spectra of **Mo₅ox** in CD₃OD
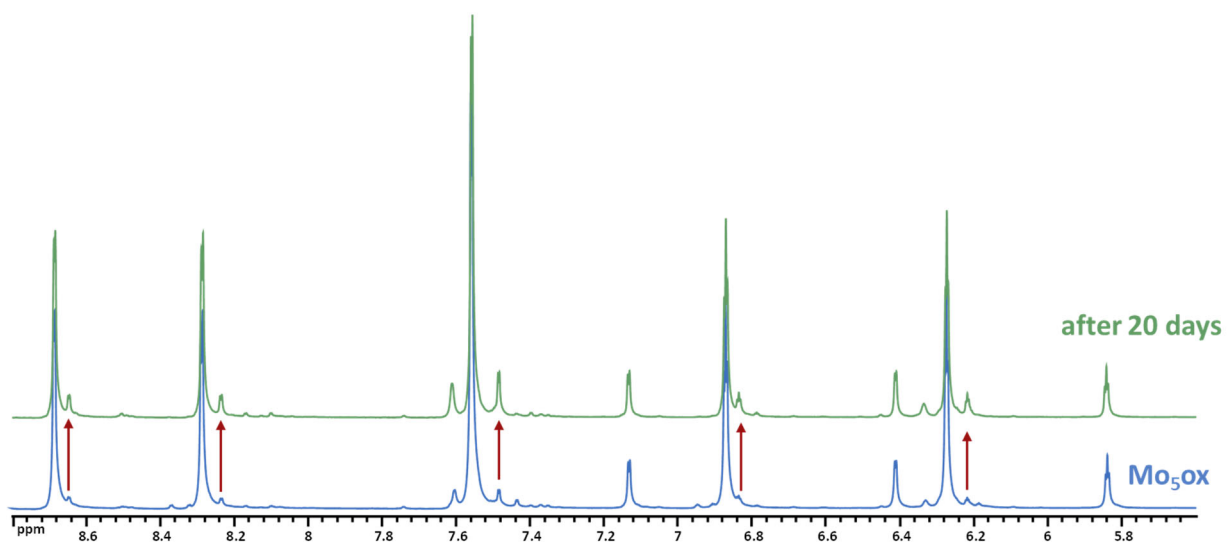
Figure S24. ^{1}H NMR spectra of **Mo₅ox** in CD₃OD in time. Red arrows indicate appearance of new signals of equatorial pyrazole and inner pyrazolate ligands.

Mass-spectrometry data
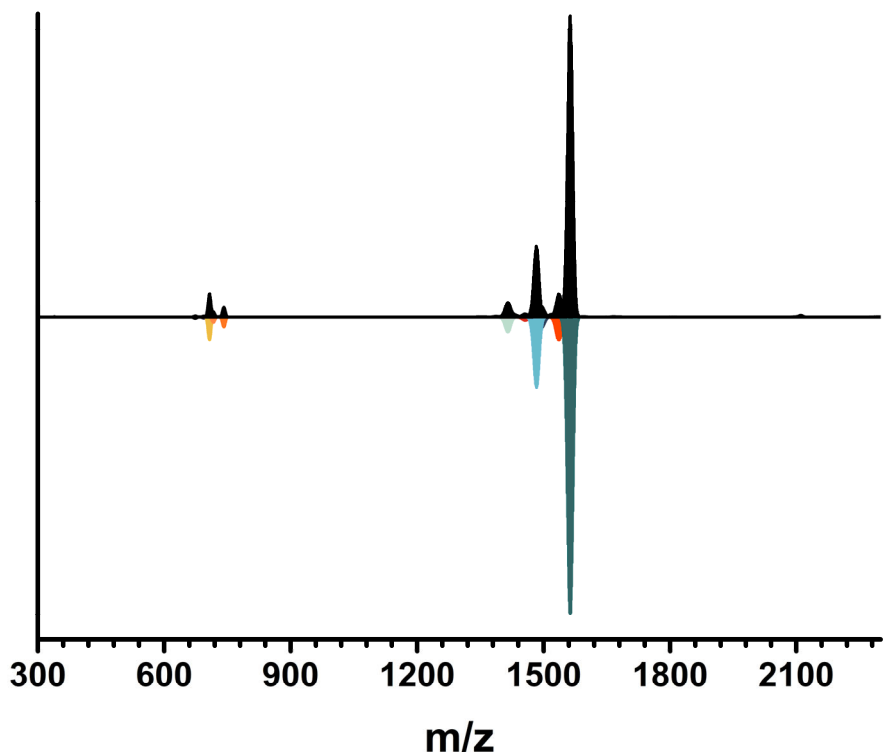
Figure S25. HR-ESI-MS spectrum of solution of **Mo$_5$ox** in acetonitrile (black) and simulations of cluster forms (colored).
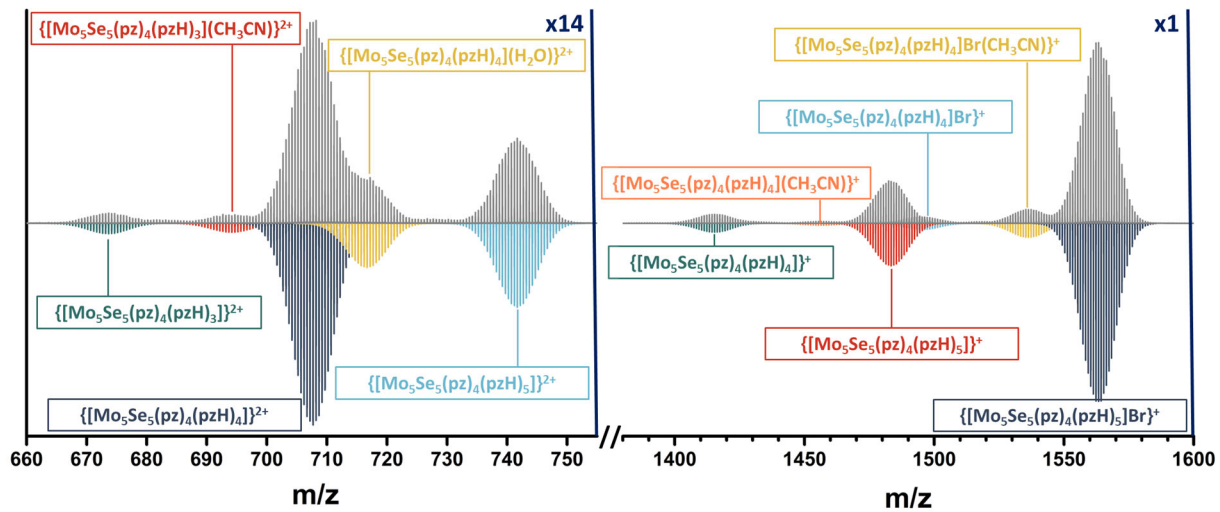

Figure S26. Fragment of HR-ESI-MS spectrum of solution of **Mo$_5$ox** in acetonitrile (gray) and simulations of cluster forms (colored).

EPR spectroscopy data
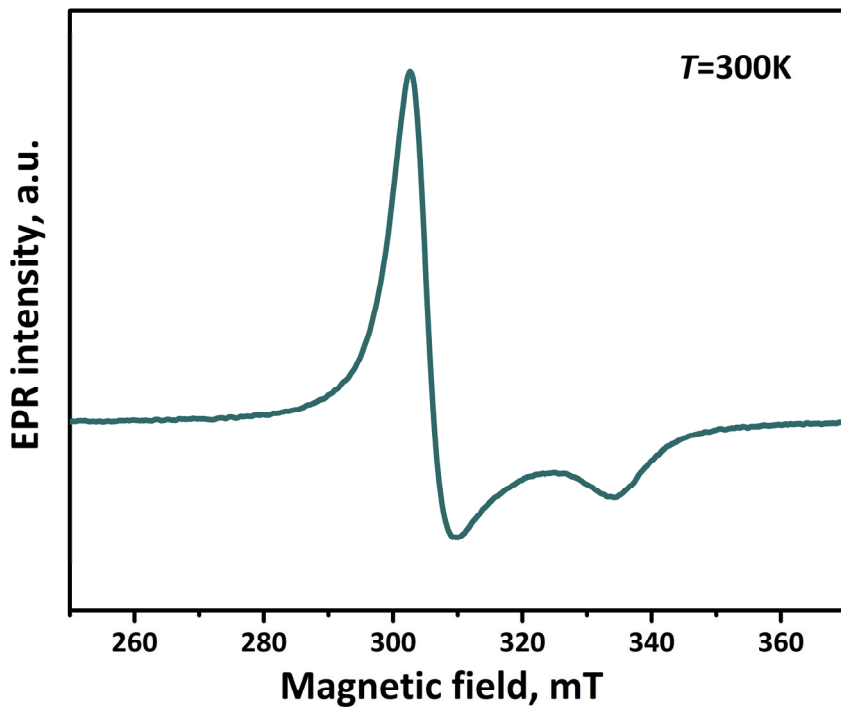
Figure S27. EPR spectrum of **Mo₅red** at 300 K. The g-tensor values are evaluated to be $g_{xx} = g_{yy} = 2.19$ and $g_{zz} = 1.99$ ($g_{iso} = 2.12$) changing slightly with temperature.
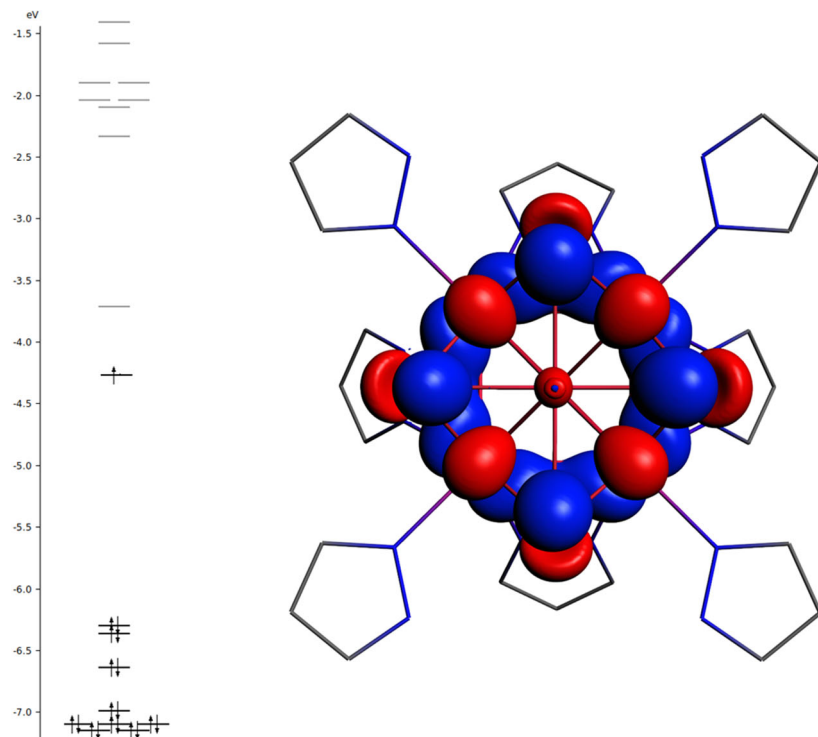
**Figure S28.** The HOMO orbital of the $[\{Mo_5(\mu_3\text{-}Se)_4(\mu_4\text{-}Se)(\mu\text{-}pz)_4\}(pzH)_5]^+$ cation. The hydrogen atoms are omitted for clarity, the isosurface value is 0.035, view along the [001].
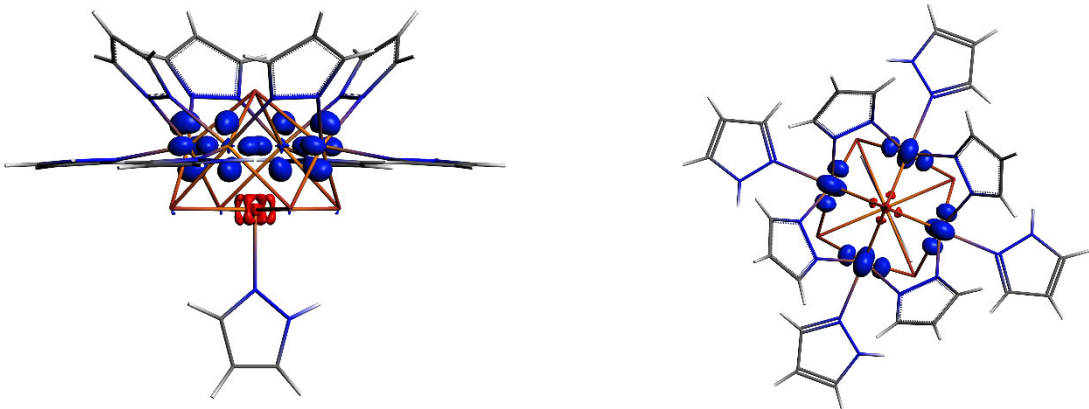
Figure S29. The plot of the spin density in the [{Mo$_5$(µ$_3$-Se)$_4$(µ$_4$-Se)(µ-pz)$_4$}(pzH)$_5$]$^+$ cation. The isosurface value 0.01, view along the [100] (left) and [001] (right). The spin density distribution in general corresponds to the *d*-orbitals of the basal Mo atoms.

Cyclic voltammetry data
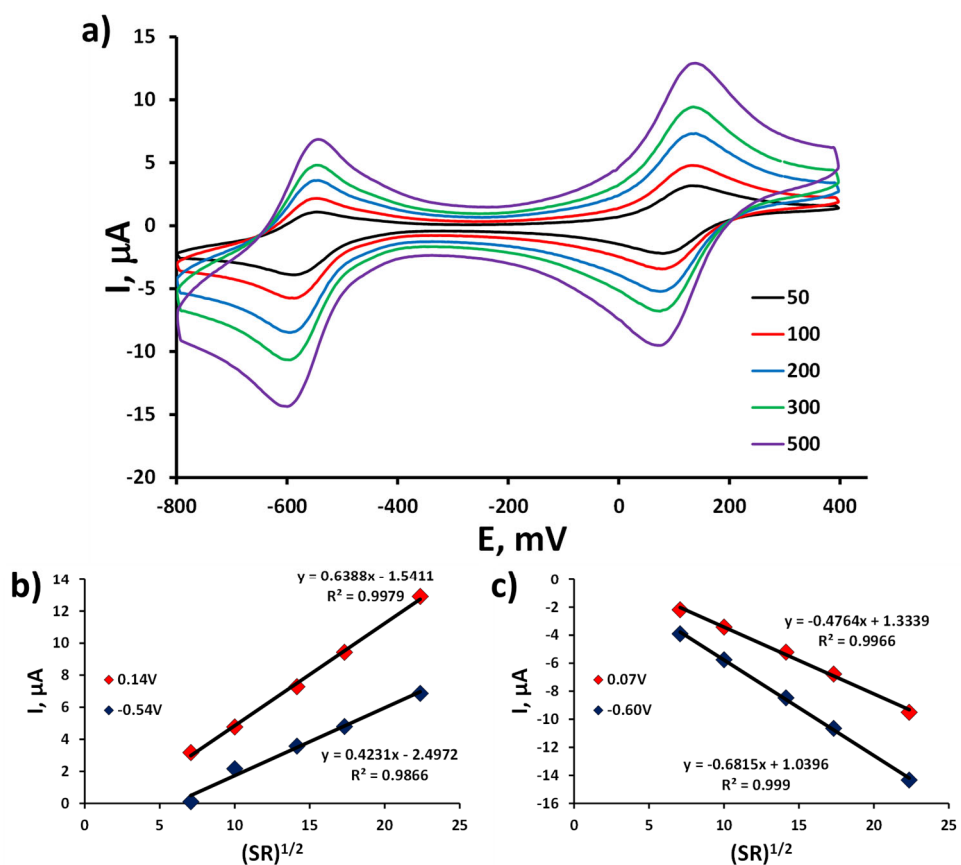
Figure S30. Cyclic voltammetry of the **Mo₅red** (0.5 mM) in 0.1 M Bu₄NClO₄ acetonitrile solution at different scan rates (a). Linear dependence of the anodic (b) and cathodic (c) peak current upon square root of the potential scan rate $\sqrt{SR}$;
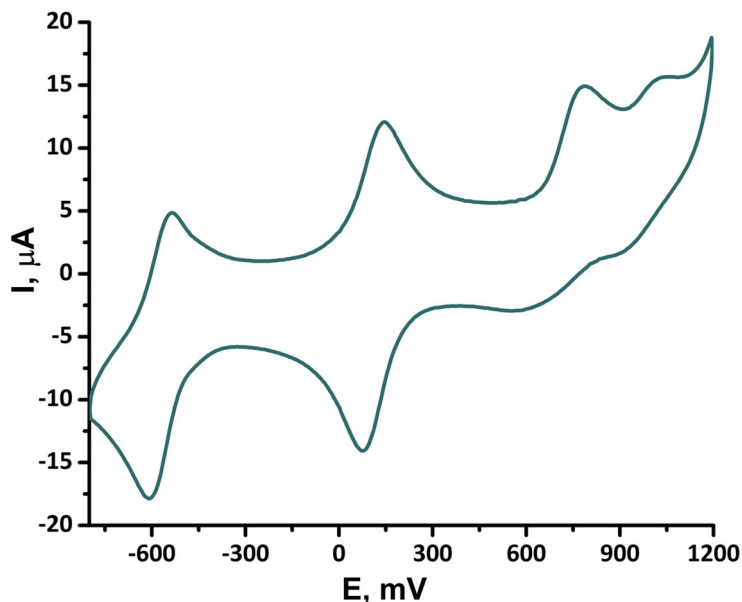
Figure S31. Cyclic voltammetry of the **Mo₅red** (0.5 mM) in 0.1 M Bu₄NClO₄ acetonitrile solution.

# Characterization of compounds: IR spectra, TGA curves, UV-vis spectra and PXRD data
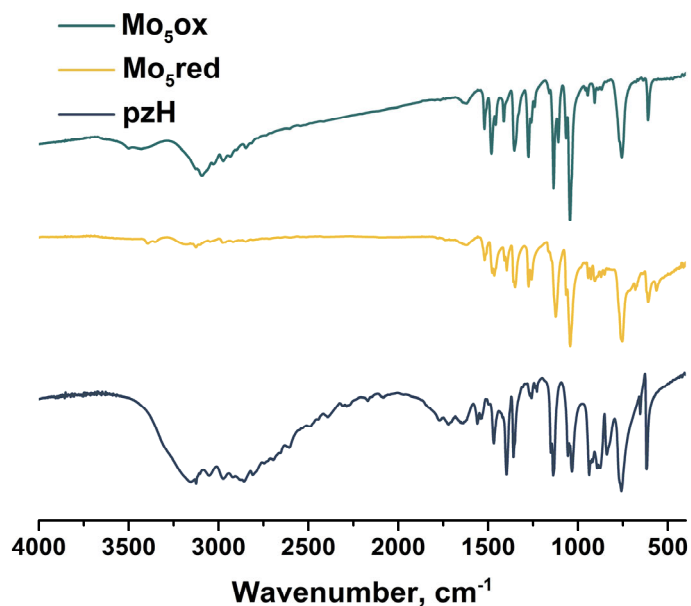
Figure S32. FTIR spectra of **Mo₅red** and **Mo₅ox** in comparison with pyrazole.
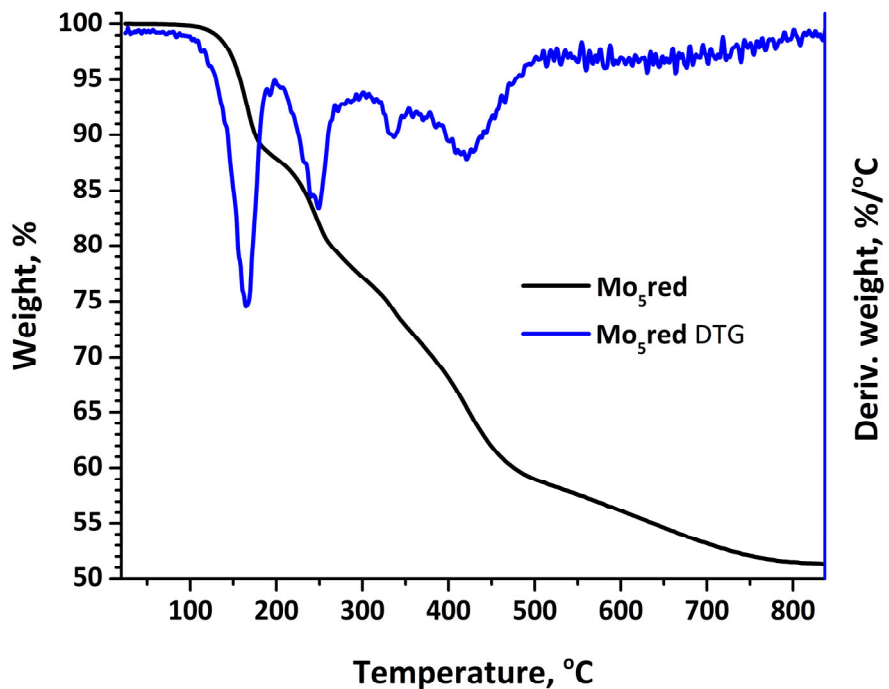
Figure S33. TGA and DTG curves of **Mo₅red**. Heating rates of 10 °C·min⁻¹.
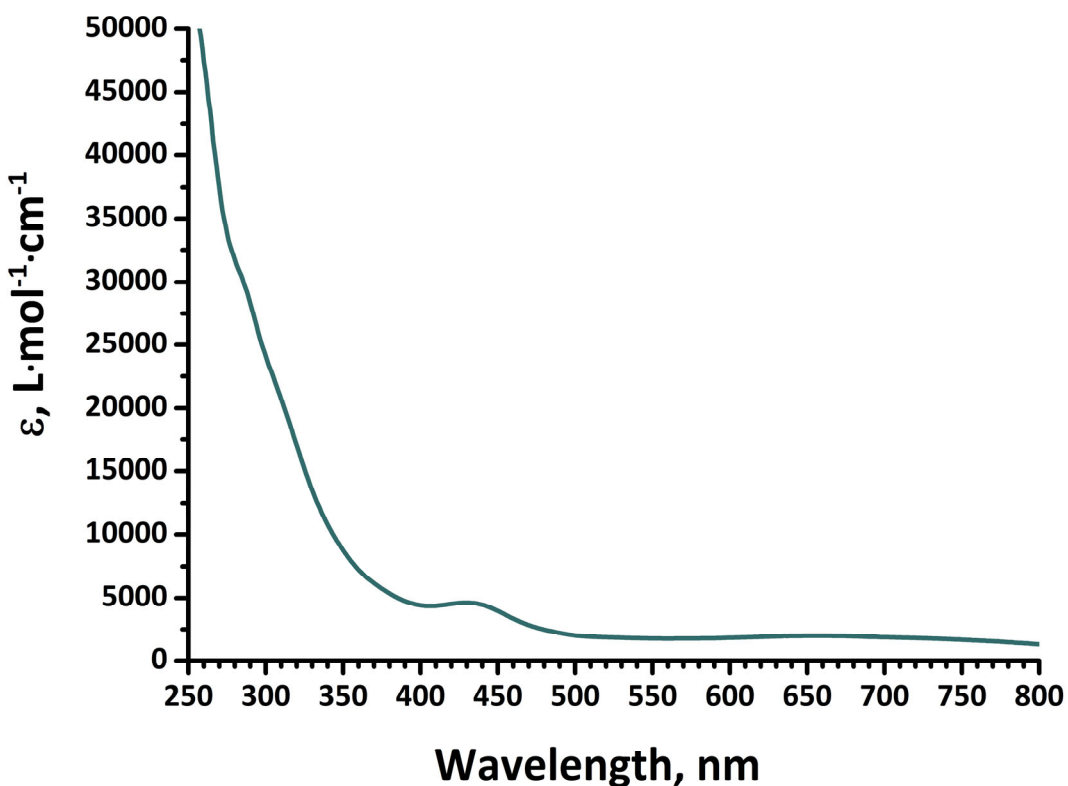
Figure S34. UV-vis spectrum of **Mo$_5$red** acetonitrile solution.
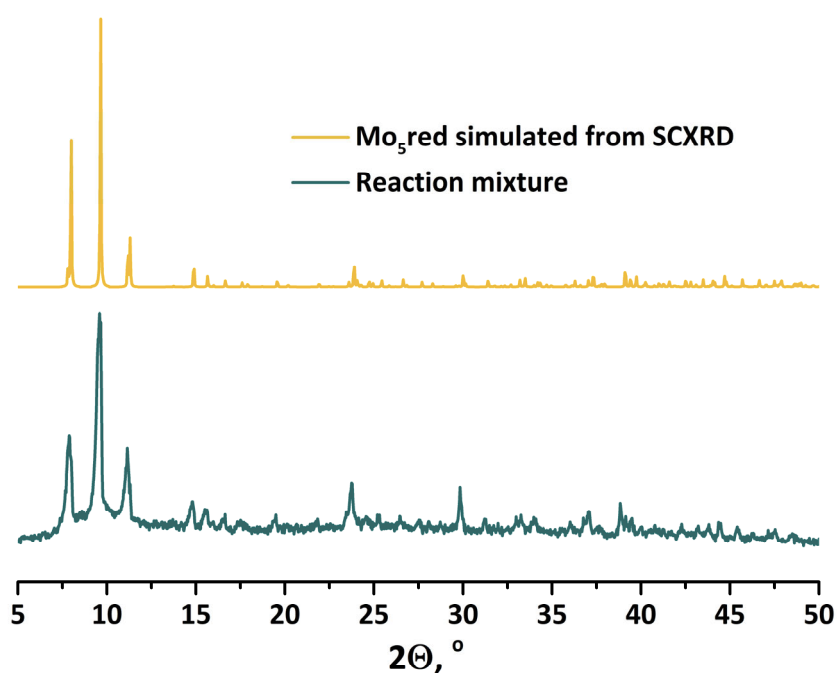
Figure S35. XRPD pattern of reaction mixture in comparison with calculated one from the SCXRD data for **Mo$_5$red**.
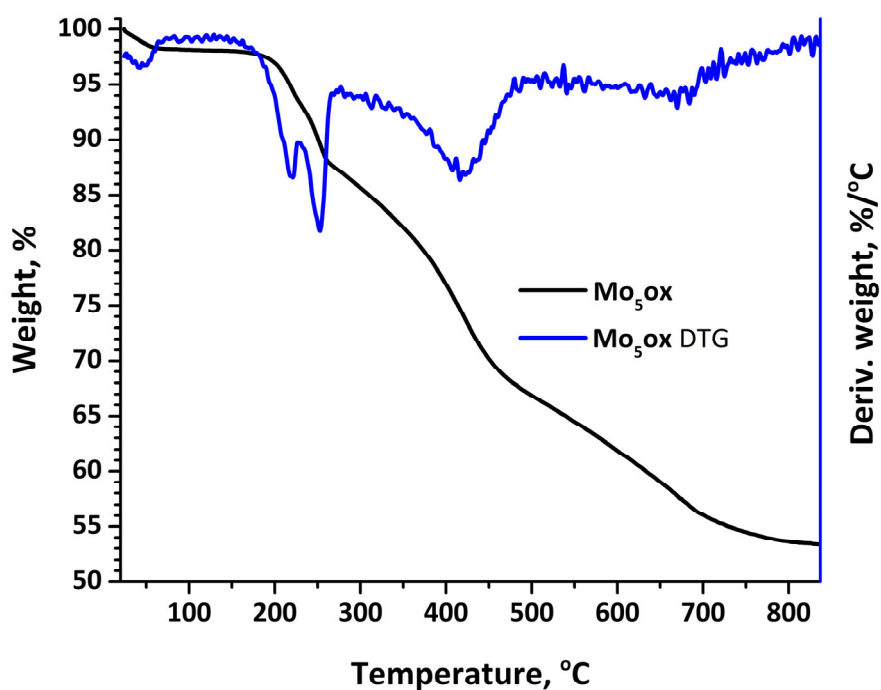
**Figure S36.** TGA and DTG curves of **Mo₅ox**. Heating rates of 10 $^{\circ}$C·min^{-1}.
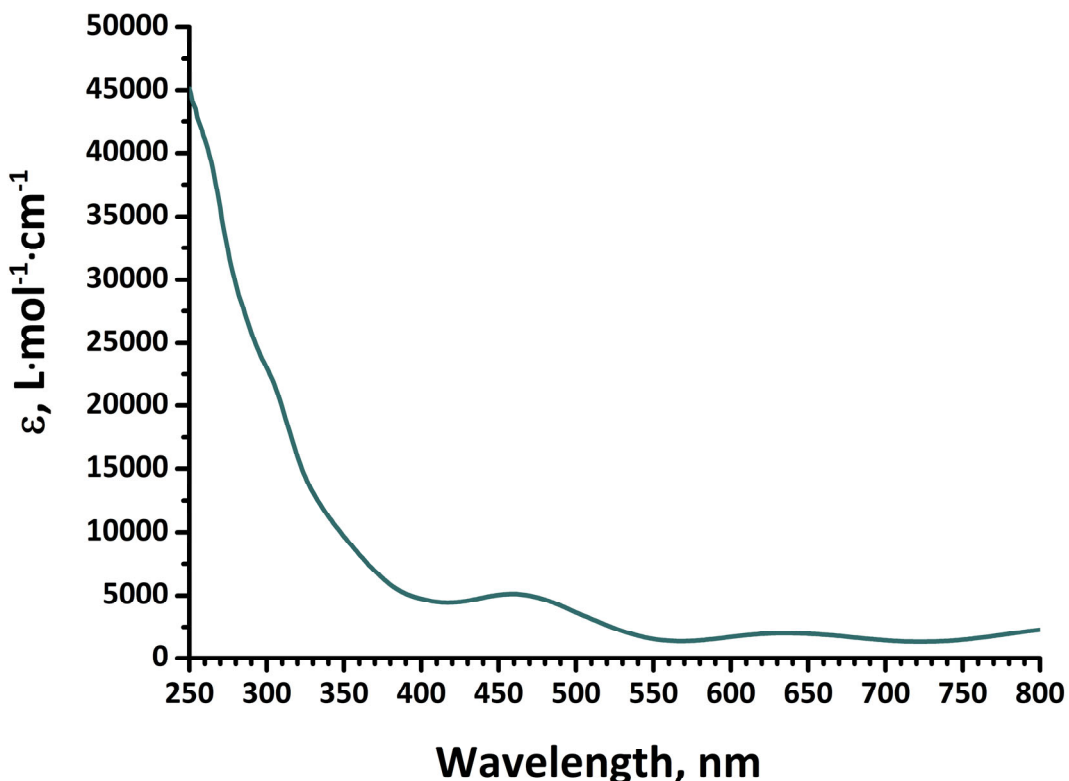
**Figure S37**. UV-vis spectrum of **Mo₅ox** acetonitrile solution.

Crystal structure data

Table S4. Selected crystallographic parameters of the single-crystal X-ray diffraction structural analysis for [{Mo$_5$(μ_3-Se)$^i_4$(μ_4-Se)^i(μ-pz)$^i_4$}(pzH)$^a_5$]Br 4pzH (**Mo$_5$red**), [{Mo$_5$(μ_3-Se)$^i_4$(μ_4-Se)^i(μ-pz)$^i_4$}(pzH)$^a_5$]Br$_2$ 2H$_2$O (**Mo$_5$ox**).

Compound	Mo$_5$red	Mo$_5$ox
Empirical formula	C$_{39}$H$_{48}$BrMo$_5$N$_{26}$Se$_5$	C$_{27}$H$_{36}$Br$_2$Mo$_5$N$_{18}$O$_2$Se$_5$
Formula weight	1835.44	1679.06
Temperature, K	150(2)	150(2)
Crystal system	Tetragonal	Orthorhombic
Space group	$P4$/n	$C222_1$
a, Å	15.6443(4)	15.6320(10)
b, Å	15.6443(4)	25.5634(15)
c, Å	11.3058(2)	12.2766(8)
α, °	90	90
β, °	90	90
γ, °	90	90
V, Å^3	2767.03(15)	4905.8(5)
Z	2	4
ρ_{calc}, g/cm^3	2.203	2.273
μ, mm^{-1}	5.171	6.629
F (000)	1758	3160
Crystal size	0.22 × 0.15 × 0.12	0.21 × 0.15 × 0.12
2Θ range for data collection, °	1.801 to 28.298	2.255 to 27.256
Index ranges	$-20 \leq h \leq 19$	$-18 \leq h \leq 20$
	$-20 \leq k \leq 20$	$-32 \leq k \leq 32$
	$-15 \leq l \leq 9$	$-15 \leq l \leq 15$
Reflections collected	21000	20573
Independent reflections	3441 [R$_{int}$ = 0.0251]	5450 [R$_{int}$ = 0.0433]
Data/restraints/parameters	3441/0/183	5450/12/293
Goodness-of-fit on F^2	1.053	1.064
R_1 / wR_2(I > 2σ(I))	0.0197/0.0493	0.0331/0.0814
R_1 / wR_1 (all data)	0.0233/0.0506	0.0462/0.0852
Δρ$_{max}$/Δρ$_{min}$ (e·Å^{-3})	1.282/−1.362	0.913/−0.715